

See discussions, stats, and author profiles for this publication at: <https://www.researchgate.net/publication/235773410>

Adhesion of Mussel Foot Protein-3 to TiO₂ Surfaces: the Effect of pH

ARTICLE in BIOMACROMOLECULES · MARCH 2013

Impact Factor: 5.75 · DOI: 10.1021/bm301908y · Source: PubMed

CITATIONS

43

READS

31

6 AUTHORS, INCLUDING:



Jing Yu

University of California, Santa Barbara

29 PUBLICATIONS 504 CITATIONS

SEE PROFILE



Wei Wei

University of California, Santa Barbara

35 PUBLICATIONS 493 CITATIONS

SEE PROFILE



Jacob Israelachvili

University of California, Santa Barbara

282 PUBLICATIONS 19,719 CITATIONS

SEE PROFILE

Adhesion of Mussel Foot Protein-3 to TiO_2 Surfaces: the Effect of pH

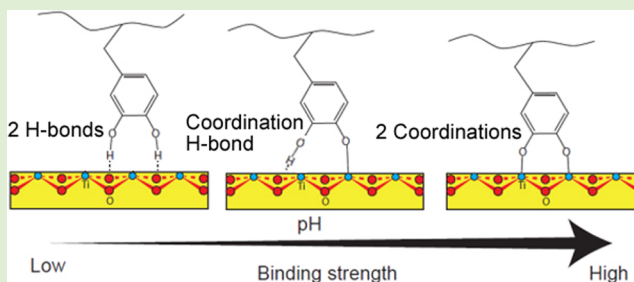
Jing Yu,^{†,‡} Wei Wei,^{†,§} Matthew S. Menyo,^{||} Admir Masic,[⊥] J. Herbert Waite,^{*,§,#} and Jacob N. Israelachvili^{‡,§}

Departments of [†]Chemical Engineering, [§]Materials Research Laboratory, ^{||}Biomolecular Science and Engineering, and [#]Molecular, Cell and Developmental Biology, University of California, Santa Barbara, California 93106, United States

[⊥]Department of Biomaterials, Max Planck Institute for Colloids and Interfaces, 14424 Potsdam-Golm, Germany

Supporting Information

ABSTRACT: The underwater adhesion of marine mussels relies on mussel foot proteins (mfps) rich in the catecholic amino acid 3,4-dihydroxyphenylalanine (Dopa). As a side chain, Dopa is capable of strong bidentate interactions with a variety of surfaces, including many minerals and metal oxides. Titanium is among the most widely used medical implant material and quickly forms a TiO_2 passivation layer under physiological conditions. Understanding the binding mechanism of Dopa to TiO_2 surfaces is therefore of considerable theoretical and practical interest. Using a surface forces apparatus, we explored the force–distance profiles and adhesion energies of mussel foot protein 3 (mfp-3) to TiO_2 surfaces at three different pHs (pH 3, 5.5 and 7.5). At pH 3, mfp-3 showed the strongest adhesion force on TiO_2 , with an adhesion energy of $\sim -7.0 \text{ mJ/m}^2$. Increasing the pH gives rise to two opposing effects: (1) increased oxidation of Dopa, thus, decreasing availability for the Dopa-mediated adhesion, and (2) increased bidentate Dopa-Ti coordination, leading to the further stabilization of the Dopa group and, thus, an increase in adhesion force. Both effects were reflected in the resonance-enhanced Raman spectra obtained at the three deposition pHs. The two competing effects give rise to a higher adhesion force of mfp-3 on the TiO_2 surface at pH 7.5 than at pH 5.5. Our results suggest that Dopa-containing proteins and synthetic polymers have great potential as coating materials for medical implant materials, particularly if redox activity can be controlled.



INTRODUCTION

Mussels have mastered the art of wet adhesion, producing a bundle of threads tipped with adhesive pads, known collectively as the byssus, which serves as a robust holdfast in the often-treacherous environment of the intertidal zone. The byssus consists of a suite of proteins having distinct localization and function, but united by the presence of the unusual modified amino acid 3,4-dihydroxyphenylalanine (Dopa). Mussel foot protein-3 *fast* (mfp-3f), a primary adhesive protein located at the plaque/substrate, has a Dopa content of 20 mol % and has been shown to exhibit remarkable adhesive properties to mica surfaces.¹

The ability of Dopa to bind to surfaces with wide-ranging chemical and physical properties has inspired much research dedicated to understanding the mechanism of mussel adhesion^{1,2} as well as developing biomimetic adhesives for underwater and medical as well as dental applications.³ Titanium is widely used in medical implant devices. A 2–20 nm thick TiO_2 passivation layer is rapidly formed on titanium under physiological conditions, yielding a hydroxyl-terminated surface that is vital in promoting biocompatibility.⁴ Therefore, study of the interaction between Dopa-containing proteins/polymers and TiO_2 substrates is of particular interest.

Dopa has a strong binding affinity to a variety of metal oxide surfaces due to the stable bidentate modes of H-bonding and metal coordination,⁵ therefore, Dopa containing proteins and polymers have great potential as molecular anchors of coatings on metal oxide surfaces. The coordination chemistry of Dopa/catecholic compounds has been studied extensively.⁶ AFM tests have shown that the pull-off of a single Dopa residue adsorbed to a wet titania surface requires a breaking force of nearly 1 nN and is completely reversible.² Strong adhesion forces have also been reported by recent SFA tests of Dopa-grafted peptides and mfp-1 on TiO_2 substrates.^{3a,7}

Density functional theory studies have shown that the binding of a Dopa group to a TiO_2 surface involves at least three different forms: molecular adsorption (through H-bond), partially dissociated monodentate adsorption, and fully dissociated bidentate adsorption.⁸ In aqueous solutions, depending on the pH of the solution, either form of binding can be the dominating binding mechanism. At relatively low pH, $\text{pH} < 5.5$, the Dopa group is not ionized, with the two hydroxyl groups preferring to form two hydrogen bonds with

Received: December 20, 2012

Revised: February 11, 2013

Published: March 4, 2013

the O atoms of the substrate. At higher pH (usually $\text{pH} \geq 8$) and in the presence of appropriate metal ions, both hydroxyl groups undergo some degree of dissociation: the first because pH is approaching the pK_a (9.8 for Dopa),⁹ and the second because of the inductive effects of metal binding. The two phenolic O atoms form two coordination bonds (a charge-transfer complex with certain metals) with surface-bound, available Ti (Ti^{IV}) sites. At an intermediate pH, a combination of one hydrogen bond and one coordination bond may be formed, resulting in a monodentate adsorption. The binding strength of a Dopa– TiO_2 coordination bond (~ 44 kT) is significantly stronger than the Dopa–Ti hydrogen bond (~ 4 – 12 kT).¹⁰ Therefore, the binding of a single Dopa to TiO_2 substrate is much stronger at pH 7.5 than at pH 3.

Resonance Raman spectroscopy has proven to be a powerful tool to observe and probe the mechanism and configuration of Dopa-metal coordination.^{3b,6,11} Mfp-1 and Dopa-grafted synthetic polymers were shown to form stable bis- and triscatecholate complexes with Fe(III) at pH 7.5 or higher in vitro and in situ (in the mussel plaque).^{3b,11,12} Resonance-enhanced signals assigned to mono- and bidentate coordination were seen for a Dopa-containing protein on TiO_2 .⁶ Despite having excellent binding ability to mica and TiO_2 surfaces, Dopa has a confounding tendency that presents significant challenges to many potential applications: at alkaline pH and with trace oxidants such as O_2 , Dopa can readily undergo a two-electron oxidation to dopaquinone, which greatly diminishes the adhesion of mfp-3f to mica.^{1a} Mussels have evolved a strategy to minimize Dopa oxidation by combining an acidic pH, imposed during the formation of the mussel plaque, with the cosecretion of an antioxidant protein, mfp-6. Mussels also use the Dopa– Fe^{3+} coordination complex to temporarily stabilize the Dopa in the plaques.^{11,13} According to AFM single molecule studies, Dopa oxidation to dopaquinone reduces binding to a TiO_2 surface by 80%, which indicates that Dopa oxidation could also strongly perturb adhesion of mussel foot proteins to TiO_2 or other metal oxide surfaces. Although much attention has been paid to engineering mussel mimetic functional coating materials, few if any studies have systematically examined the effect of Dopa oxidation on the performance of those coating materials on metal oxide surfaces.

To remedy this oversight, we investigated the adhesion of mfp-3f to TiO_2 surfaces (RMS ~ 1 nm, Figures S1 and S2). SFA force measurements and resonance Raman spectroscopic investigations into the binding of mfp-3f on TiO_2 surfaces indicate that, although higher pH leads to increased Dopa oxidation, it also significantly increases the adhesion of surviving Dopa in mfp-3f on TiO_2 surfaces.

EXPERIMENTAL SECTION

Protein Purification. Purification of mfp-3f was achieved exactly as previously described.¹⁴ The purified proteins were suspended in buffer consisting of 0.1 M acetic acid (EMD Chemicals, Gibbstown, NJ), and 0.25 M potassium nitrate (Aldrich, St. Louis, MO) and with a pH of 3. The protein solutions were divided into small aliquots and stored at -50°C before experiments.

Surface Forces Apparatus. The adhesion of mfp-3f on TiO_2 surfaces was studied using a surface forces apparatus 2000 (SFA 2000) with a reported geometry.¹⁵ A 10 nm thick TiO_2 layer was deposited on the mica surfaces glued on the SFA disks using an E-Beam deposition method (Temescal system) at a constant rate of 0.1 nm/s and a pressure $< 4 \times 10^{-5}$ Torr and was shown to be free of impurities by XPS (Kratos Ultra, Kratos Analytical Limited, S Figure 1). The surface roughness of the TiO_2 substrate was 1 nm measured by AFM

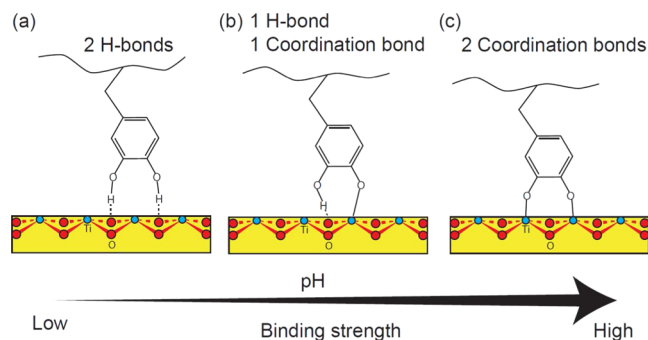


Figure 1. Possible modes of Dopa (catechol) binding to nonhydrated TiO_2 surfaces. The catechol group can form molecular adsorption with (a) two hydrogen bonds, (b) monodentate adsorption with one hydrogen bond and one coordination bond, and (c) bidentate adsorption with two coordination bonds, although which form the Dopa binds to a TiO_2 surface depends is pH-dependent: at lower pH ($\text{pH} < 5.5$), the molecular adsorption is preferred, and at higher pH ($\text{pH} > 7$), the coordination charge transfer is more favorable. As marked, the red atoms are oxygens and the blue ones are titanium.

(Asylum MFP-3D-SA, S Figure 2). Prior to experiments, a droplet of mfp-3f solution with a mfp-3 concentration of $5\ \mu\text{g/mL}$ ($\text{pH} = 3$) was

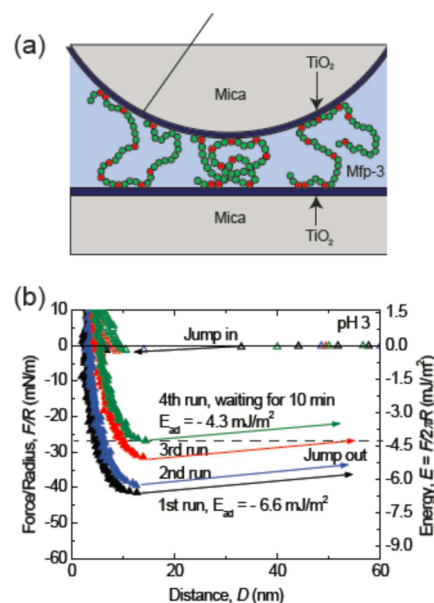


Figure 2. (a) Geometry of SFA experiments (Dopa residues in red). (b) Adhesion of mfp-3 on TiO_2 surface in pH 3 buffer decreases with the force cycles/experiment time. The adhesion force dropped about 40% in about 1 h. This is probably due to the light-induced oxidation of Dopa on TiO_2 .¹³

pipetted on top of one TiO_2 surface, letting the protein adsorb for 20 min and ideally forming a monolayer of mfp-3 molecules on the surface. The TiO_2 surfaces were then rinsed thoroughly with pH 3 buffer (0.1 M acetic acid, 0.25 M potassium nitrate, Sigma Aldrich) to remove the unabsorbed protein and then mounted into a SFA box. Buffer change was achieved by repeated injection and removal of buffer between the two surfaces. The distance D between two surfaces is measured with an optical interferometry technique (fringes of equal chromatic order, FECCO). By applying the Derjaguin approximation, the normalized force F/R between the two cylindrical SFA surfaces is directly proportional to the energy between two flat surfaces with a simple relation of $E(D) = F(D)/2\pi R$. Buffer preparation: 0.1 M sodium acetate (EM Science, Gibbstown, NJ) and 0.25 M potassium

nitrate titrated by acetic acid (pH 5.5); 0.016 M potassium phosphate monobasic (Mallinckrodt, Hazelwood, MO) and 0.084 M potassium phosphate dibasic (EMD Chemicals, Gibbstown, NJ; pH 7.5). Milli-Q water (Millipore, Bedford, MA) was used for all the glassware cleaning and solution preparation.

Raman Spectroscopy. Raman spectra were collected with a confocal Raman microscope ($\alpha 300$; WITec) equipped with a Nikon objective (100 \times) and a laser excitation wavelength of 532 nm. Spectra were acquired with a CCD camera (DV401-BV; Andor) behind a spectrometer (UHTS 300; WITec) with a spectral resolution of 3 cm^{-1} . Samples were prepared by drop-casting 20 μL of mfp-3f solution (10 $\mu\text{g}/\text{mL}$) in the appropriate buffer solution onto the TiO_2 -coated mica surfaces described for the SFA experiments, followed by incubation under ambient conditions for 20 min. After adsorption, surfaces were rinsed with the respective buffer solution and dried with a stream of N_2 . Samples were sensitive to burning by the laser beam; therefore, laser power was restricted to 10–20 mW. Each collected spectrum consisted of 120 accumulations; with an integration time of 1 s. ScanCtrlSpectroscopyPlus software (version 1.38, Witec) was used for measurement setup. The acquired spectra were analyzed and processed with Witec Project software (version 2.08). Spectra were background subtracted (average background subtract function) and smoothed with a 9-point Savitzky-Golay filter (fourth order polynomial). Background spectra of TiO_2 -coated mica substrate with and without drop-cast buffer solution were also collected.

RESULTS AND DISCUSSION

Adhesion of mfp-3f on TiO_2 Surfaces at Different pHs.

We have used the surface forces apparatus (SFA) to investigate adhesive interactions between mfp-3f and TiO_2 at three pHs. As only monolayers of mfp-3f are deposited on TiO_2 , we can focus completely on their surface interactions. Cohesive changes resulting from protein cross-linking due to quinone formation arise primarily when multiple protein layers are present on the surfaces tested in the SFA. Strongest adhesion force with a corresponding adhesion energy of $-6.6 \text{ mJ}/\text{m}^2$ was measured at pH 3 after a brief compression of 1 min followed by separation of two surfaces. The thin hard wall ($\sim 5 \text{ nm}$) of the force profile indicates that only a monomolecular layer of mfp-3f was deposited on the surface. Apparently, during contact, the mfp-3f molecules preadsorbed onto one TiO_2 surface can span the gap to bind to another surface, which gives rise to strong bridging adhesion. Interestingly, the adhesion force measured at pH 3 was not stable, showing strong time dependence. The adhesion force decreased with increasing the approach/separation force run cycles and the time of the experiment. In the third force run, the adhesion energy measured dropped to $-5 \text{ mJ}/\text{m}^2$, about 25% decrease of the initial adhesion. Unlike on mica surfaces, a longer contact time did not enhance the adhesion force of mfp-3 on TiO_2 surfaces: in the fourth force run, we kept the surfaces in contact for 10 min, and the adhesion force measured during separation decreased to $-4.5 \text{ mJ}/\text{m}^2$.

The decrease in adhesion forces is probably due to the oxidation of Dopa on a TiO_2 surface that is subjected to strong light intensity. Dopa does not undergo oxidation at pH 3 in bulk solution; however, TiO_2 is a good photo-oxidation catalyst.¹⁶ In the SFA, strong white light is used with the interferometric analyses of separation and force. Under such conditions, TiO_2 can easily oxidize the Dopa group into dopaquinone, which greatly diminishes the adhesion of Dopa to TiO_2 . Although the effect of photo-oxidation was very significant in our SFA tests, it is probably irrelevant to medical coatings applications because exposure to intense light is not typically involved in those processes.

The strong initial adhesion of mfp-3f on TiO_2 surfaces at pH 3 dropped significantly to $-0.7 \text{ mJ}/\text{m}^2$ when the gap solution pH was increased to pH 5.5 (Figure 3a). Previous SFA studies

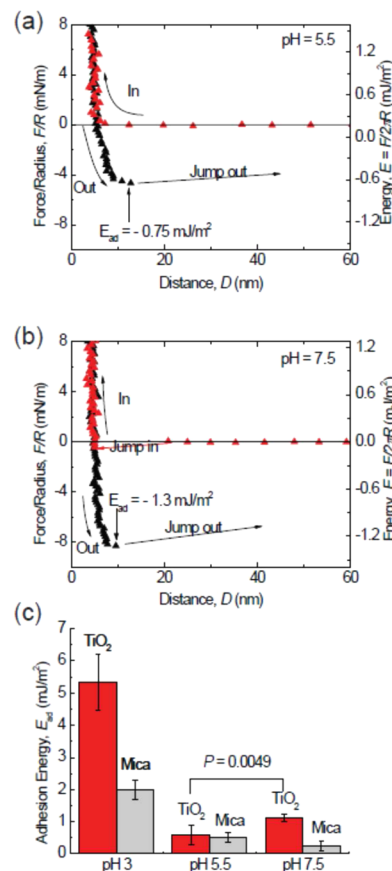


Figure 3. pH dependence of adhesion of mfp-3f to TiO_2 . Reduced adhesion occurs upon increasing the pH to 5.5 (a). A surprising increase in adhesion by almost 40% occurs upon bringing the pH up to 7.5 (b). Although Dopa loss to oxidation is more severe at high pH, the Dopa– TiO_2 coordination bond gives higher adhesion forces. (c) A summary of the adhesion energies of mfp-3 on TiO_2 in different pH buffers. The adsorption of Dopa on TiO_2 surface is highly pH-dependent. At low pH, the protonated Dopa predominates, whereas at pH 7.5, there exists a mixture of both half- and fully deprotonated catecholates.

on mica surfaces have shown similar trends, due to the auto-oxidation of Dopa to dopaquinone at high pH. Dopaquinone participates only weakly in all three types of adsorption, thereby auto-oxidation can greatly reduce the adhesion of mfp-3f to TiO_2 surface.¹ Surprisingly, increasing the pH to 7.5 did not further reduce adhesion, but instead increased it to $-1.3 \text{ mJ}/\text{m}^2$. Given that Dopa is more susceptible to auto-oxidation at pH 7.5, there should be fewer Dopa groups available for binding and correspondingly lower adhesion; however, increasing the pH also increases the possibility of monodentate or bidentate binding of Dopa to the TiO_2 surfaces,^{7,8,17} thereby leading to much stronger binding than the molecular absorption through hydrogen bonds at the single molecular level. Ti^{IV} -complexation by coordination may also significantly improve the stability of Dopa, as shown in mussel plaques. As a result of the two competing effects, the adhesion of mfp-3f on TiO_2 surface is stronger at pH 7.5 than at pH 5.5.

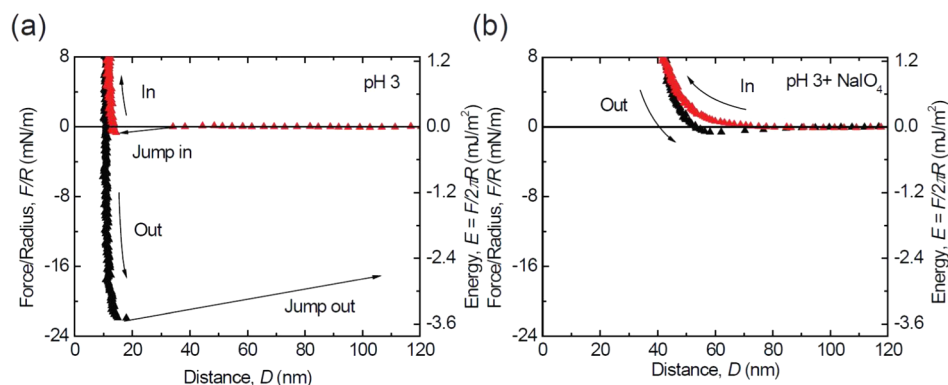


Figure 4. Periodate treatment as an independent measure of the effect of Dopa oxidation on adhesion. At pH 3, before adding periodate, strong adhesion was measured (a). The adhesion is almost completely abolished (96% decrease) by adding periodate at pH 3 (b).

To explore the correlation between the loss of adhesion and Dopa oxidation, we performed a control Dopa oxidation experiment using an oxidant, periodate, at pH 3, where the strongest adhesion was detected. After achieving a final stable adhesion energy of -3.6 mJ/m^2 , $20 \mu\text{L}$ of periodate solution ($100 \mu\text{M}$) was injected into the gap between the surfaces (Figure 4). Only weak adhesion, corresponding to an energy of -0.15 mJ/m^2 , was detected in the separation after driving two surfaces into contact. The periodate oxidation experiment supports our proposition that oxidation of Dopa to dopaquinone decreases mfp-3f adhesion to mica at pH 5.5 and 7.5, however, it does not preclude the possibility that electrostatic attraction also contributes to the increased adhesion at pH 7.5. The 4-fold increase in the hardwall (from 10 to 40 nm) has been attributed to the effect of dehydroDopa formation on backbone stiffening and is typically reversible with reduction.¹

Raman Spectroscopy Study. To further investigate the binding mechanism of mfp-3f to TiO_2 , we performed Raman spectroscopy measurements on mfp-3f adsorbed on TiO_2 surfaces at three different pHs (pH 3, 5.5, and 7.5). Figure 5 shows background-subtracted Raman spectra for mfp-3f adsorbed at pH 3 and 5.5, normalized to the nonresonant CH vibrational peak ($2800\text{--}3000 \text{ cm}^{-1}$; Figure S3). The spectrum for protein adsorption at pH 7.5 is shown in the Supporting Information (Figure S4). Prominent peaks in the spectrum resulting from mfp-3f deposition at pH 5.5 are consistent with those seen for mfp-1– TiO_2 adsorption and share marked similarity to those originating from the complexation of mfp-1 and Fe^{3+} .^{3b,6,11} Low energy resonance peaks ($500\text{--}700 \text{ cm}^{-1}$) have previously been assigned to vibrations of the oxygen–metal chelate bonds. Specifically, peaks at 585 and 639 cm^{-1} indicate coordination by the oxygens on C3 and C4 of the catechol ring, respectively, whereas that of 530 cm^{-1} arises upon bidentate coordination and resulting charge transfer. Higher energy resonance peaks ($1200\text{--}1500 \text{ cm}^{-1}$) have been assigned to catechol ring vibrations.¹¹ The pronounced spectral features in this region highlight the involvement of the catechol in the interfacial charge transfer upon coordination to TiO_2 . Namely, the strong ring stretch at 1488 cm^{-1} is indicative of the formation of a catechol–Ti charge transfer complex and has previously been observed upon charge transfer following formation of tris-Dopa– Fe^{3+} complexes.^{6,11} Similarly, a strong feature at 1331 cm^{-1} , attributed to a C–O stretching mode, indicates the vital

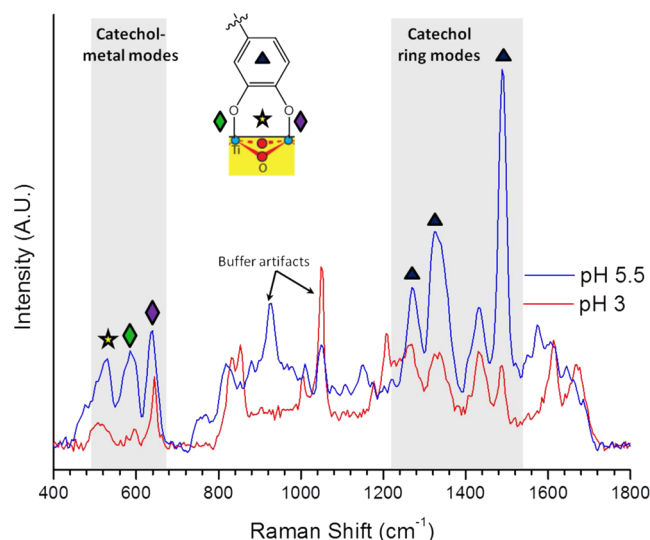


Figure 5. Resonance Raman spectra of Dopa– TiO_2 interactions in mfp-3f adsorbed at pH 3 and 5.5. Peaks at 1488 cm^{-1} (\blacktriangle ; $\nu \text{ C–C}_{\text{arom}} + \nu \text{ C–H}_{\text{arom}}$), 1329 , and 1261 cm^{-1} (\blacktriangle ; $\nu \text{ C–O} + \nu \text{ C–C}_{\text{arom}}$) are characteristic catechol peaks which are enhanced upon coordination and charge transfer. Signals at 639 cm^{-1} (\blacklozenge ; $\delta, \nu \text{ C}_4\text{–O}$), 585 cm^{-1} (\blacklozenge ; $\delta, \nu \text{ C}_3\text{–O}$), and 530 cm^{-1} (\star ; $\delta, \nu \text{ C–O}$ bidentate coordination) are characteristic catechol/metal chelate modes. Resonance enhancement of diagnostic modes for coordination is reduced at lower pH, suggesting predominant Ti–Dopa bridges at pH 5.5 and largely uncomplexed protein at pH 3. Peaks labeled represent artifacts from the buffer solutions (sodium acetate C–C at 930 cm^{-1} and nitrate $\text{N–O } \nu_1$ at 1050 cm^{-1}).¹⁹

role of the catecholate functionality in providing bridging adsorption.¹⁸

The spectra acquired at pH 3 also show characteristic enhanced signals in both the high and low energy regions shaded in Figure 3. The strength of these signals is notably diminished relative to that of mfp-3f adsorbed at pH 5.5. As anticipated, binding at pH 3 results in a suboptimal coordination, as protons outcompete surface metal sites for the catecholate anions.

Mfp-3f deposited at pH 7.5 shows a strong fluorescent background (Figure S4) that obscures all other signals; therefore, resonance-enhanced peaks signifying coordination could not be detected. However, it is anticipated that similar coordination peaks would indeed be seen at this pH, explaining

the relatively robust adhesion measured in the SFA experiments.

Taken together, the Raman spectroscopy measurements support the SFA findings: increased pH favors the possibility of coordination binding of Dopa to the TiO₂ surfaces while also increasing the rate of Dopa oxidation, which decreases the amount of Dopa residues available for binding. These opposing effects strongly alter the adhesive properties of mfp-3f and certainly have a similar effect on other Dopa-containing adhesives. This emphasizes the importance of well-controlled deposition conditions in forming robust interfacial binding. It is known that mussels regulate both the pH in the distal depression during protein secretion and the oxidation by cosecreting a protein, mfp-6, shown to have antioxidant properties at a wide range of pH. This study has confirmed the role of deposition pH on the adsorption and adhesive properties of mfp-3f to titania surfaces. Ongoing studies are geared toward the understanding of codeposition strategies that retard the rate of oxidation at high pH, thereby allowing optimal surface complexation.

Finally, it should be noted that mussels use several different variants of mfp-3 as well as other mfps for adhesion to surfaces.¹⁴ The Dopa in some of these variants exhibits significantly shifted redox properties²⁰ that could also show enhanced or altered binding to TiO₂ surfaces and should be investigated in future studies.

CONCLUSION

Understanding the binding mechanism of Dopa to TiO₂ surfaces is crucial for applying mussel-inspired polymers as coating materials on TiO₂. Our results show that mfp-3f binds strongly to TiO₂ surfaces at low pH (pH 3). Raising the pH gives rise to two opposing effects: (1) Dopa oxidation, which decreases the adhesion of mfp-3f to TiO₂ surfaces; (2) changing the binding nature of a single Dopa to the TiO₂ from H-bonding to coordination bonding and, therefore, increases the binding strength of a single Dopa group to the TiO₂ surface. The two competing effects lead to a higher adhesion of mfp-3f on TiO₂ surfaces at pH 7.5, whereas the lowest adhesion forces were measured at pH 5.5. Our results demonstrate that, by carefully controlling the Dopa redox activity, Dopa-containing proteins and synthetic polymers can strongly bind to TiO₂ surfaces, hence, offering promise as coating materials for medical implants.

ASSOCIATED CONTENT

Supporting Information

S1, XPS analysis of the TiO₂ layer; S2, A tapping mode image of the TiO₂ surface; S3, Full window Raman spectra of mfp3f on TiO₂ at pH 3 and 5.5; S4, The intrinsic fluorescence of mfp-3f following pH elevation to 7.5 and calculation of binding energy to TiO₂. This material is available free of charge via the Internet at <http://pubs.acs.org>.

AUTHOR INFORMATION

Corresponding Author

*E-mail: waite@lifesci.ucsb.edu.

Author Contributions

[†]These authors contributed equally to this work.

Notes

The authors declare no competing financial interest.

ACKNOWLEDGMENTS

This work was supported by the Materials Research Science and Engineering Centers Program of the National Science Foundation under Award No. DMR 1121053, the IMI Program of the National Science Foundation under Award No. DMR 0843934, the National Institutes of Health under Grant R01-DE018468, and the UCSB-MPG Program for International Exchange in Materials Science. The authors thank Saurabh Das for the preparation of nanodeposited TiO₂ layers onto the mica surfaces.

REFERENCES

- (1) (a) Yu, J.; Wei, W.; Danner, E.; Ashley, R. K.; Israelachvili, J. N.; Waite, J. H. Mussel protein adhesion depends on interprotein thiol-mediated redox modulation. *Nat. Chem. Biol.* **2011**, *7* (9), 588–590. (b) Yu, J.; Wei, W.; Danner, E.; Israelachvili, J. N.; Waite, J. H. Effects of interfacial redox in mussel adhesive protein films on mica. *Adv. Mater.* **2011**, *23* (20), 2362.
- (2) Lee, H.; Scherer, N. F.; Messersmith, P. B. Single-molecule mechanics of mussel adhesion. *Proc. Natl. Acad. Sci. U.S.A.* **2006**, *103* (35), 12999–13003.
- (3) (a) Anderson, T. H.; Yu, J.; Estrada, A.; Hammer, M. U.; Waite, J. H.; Israelachvili, J. N. The contribution of dopa to substrate-peptide adhesion and internal cohesion of mussel-inspired synthetic peptide films. *Adv. Funct. Mater.* **2010**, *20* (23), 4196–4205. (b) Holten-Andersen, N.; Harrington, M. J.; Birkedal, H.; Lee, B. P.; Messersmith, P. B.; Lee, K. Y. C.; Waite, J. H. pH-induced metal-ligand cross-links inspired by mussel yield self-healing polymer networks with near-covalent elastic moduli. *Proc. Natl. Acad. Sci. U.S.A.* **2011**, *108* (7), 2651–2655. (c) Kim, B. H.; Lee, D. H.; Kim, J. Y.; Shin, D. O.; Jeong, H. Y.; Hong, S.; Yun, J. M.; Koo, C. M.; Lee, H.; Kim, S. O. Mussel-inspired block copolymer lithography for low surface energy materials of teflon, graphene, and gold. *Adv. Mater.* **2011**, *23* (47), 5618–+. (d) Lee, B. P.; Messersmith, P. B.; Israelachvili, J. N.; Waite, J. H. Mussel-inspired adhesives and coatings. *Annu. Rev. Mater. Res.* **2011**, *41*, 99–132. (e) Lee, H.; Dellatore, S. M.; Miller, W. M.; Messersmith, P. B. Mussel-inspired surface chemistry for multifunctional coatings. *Science* **2007**, *318* (5849), 426–430. (f) Shao, H.; Stewart, R. J. Biomimetic underwater adhesives with environmentally triggered setting mechanisms. *Adv. Mater.* **2010**, *22* (6), 729–+. (g) Westwood, G.; Horton, T. N.; Wilker, J. J. Simplified polymer mimics of cross-linking adhesive proteins. *Macromolecules* **2007**, *40* (11), 3960–3964. (h) Stepuk, A.; Halter, J. G.; Schaetz, A.; Grass, R. N.; Stark, W. J. Mussel-inspired load bearing metal-polymer glues. *Chem. Commun.* **2012**, *48* (50), 6238–6240.
- (4) (a) Larsson, C.; Thomson, P.; Lausmaa, J.; Rodahl, M.; Kasemo, B.; Ericson, L. E. *Biomaterials* **1994**, *15*, 1062. (b) Pan, J.; Liao, H.; Leygraf, C.; Thierry, D.; Li, J. *J. Biomed. Mater. Res.* **1998**, *40*, 244.
- (5) Waite, J. H. The phylogeny and chemical diversity of quinone-tanned glues and varnishes. *Comp. Biochem. Physiol., Part B: Biochem. Mol. Biol.* **1990**, *97* (1), 19–29.
- (6) (a) Salameh, S.; Schneider, J.; Laube, J.; Alessandrini, A.; Facci, P.; Seo, J. W.; Ciacchi, L. C.; Mädler, L. Adhesion mechanisms of the contact interface of TiO₂ nanoparticles in films and aggregates. *Langmuir* **2012**, *28* (31), 11457–11464. (b) Dalsin, J. L.; Lin, L. J.; Tosatti, S.; Voros, J.; Textor, M.; Messersmith, P. B. Protein resistance of titanium oxide surfaces modified by biologically inspired mPEG-DOPA. *Langmuir* **2005**, *21* (2), 640–646. (c) Gillich, T.; Benetti, E. M.; Rakhmatullina, E.; Konradi, R.; Li, W.; Zhang, A.; Schluter, A. D.; Textor, M. Self-assembly of focal point oligo-catechol ethylene glycol dendrons on titanium oxide surfaces: adsorption kinetics, surface characterization, and nonfouling properties. *J. Am. Chem. Soc.* **2011**, *133* (28), 10940–10950. (d) Dalsin, J. L.; Hu, B. H.; Lee, B. P.; Messersmith, P. B. Mussel adhesive protein mimetic polymers for the preparation of nonfouling surfaces. *J. Am. Chem. Soc.* **2003**, *125* (14), 4253–4258.

- (7) Hwang, D. S.; Harrington, M. J.; Lu, Q. Y.; Masic, A.; Zeng, H. B.; Waite, J. H. Mussel foot protein-1 (mfp-1) interaction with titania surfaces. *J Mater Chem* **2012**, *22* (31), 15530–15533.
- (8) (a) Terranova, U.; Bowler, D. R. Adsorption of catechol on TiO₂(2) rutile (100): a density functional theory investigation. *J. Phys. Chem. C* **2010**, *114* (14), 6491–6495. (b) Liu, Y.; Dadap, J. I.; Zimdars, D.; Eisenthal, K. B. Study of interfacial charge-transfer complex on TiO₂ particles in aqueous suspension by second-harmonic generation. *J. Phys. Chem. B* **1999**, *103* (13), 2480–2486.
- (9) (a) Martin, R. B. Zwitterion formation upon deprotonation in L-3,4-dihydroxyphenylalanine and other phenolic amines. *J. Phys. Chem.* **1971**, *75*, 2657–2661. (b) Petit, L. D. Critical survey of formation constants of complexes of histidine, phenylalanine, tyrosine, L-DOPA and tryptophan. *Pure Appl. Chem.* **1984**, *56*, 247–292.
- (10) (a) Li, S. C.; Chu, L. N.; Gong, X. Q.; Diebold, U. Hydrogen bonding controls the dynamics of catechol adsorbed on a TiO₂(110). *Surf. Sci.* **2010**, *328* (5980), 882–884. (b) Valtiner, M.; Donaldson, S. H.; Gebbie, M. A.; Israelachvili, J. N. Hydrophobic forces, electrostatic steering, and acid-base bridging between atomically smooth self-assembled monolayers and end-functionalized PEGolated lipid bilayers. *J. Am. Chem. Soc.* **2012**, *134* (3), 1746–1753. (c) Israelachvili, J. N. *Intermolecular and Surface Forces*, 3rd ed.; Academic Press: Burlington, MA, 2011.
- (11) Harrington, M. J.; Masic, A.; Holten-Andersen, N.; Waite, J. H.; Fratzl, P. Iron-clad fibers: a metal-based biological strategy for hard flexible coatings. *Science* **2010**, *328* (5975), 216–220.
- (12) Zeng, H. B.; Hwang, D. S.; Israelachvili, J. N.; Waite, J. H. Strong reversible Fe(3+)-mediated bridging between dopa-containing protein films in water. *Proc. Natl. Acad. Sci. U.S.A.* **2010**, *107* (29), 12850–12853.
- (13) Hwang, D. S.; Zeng, H. B.; Masic, A.; Harrington, M. J.; Israelachvili, J. N.; Waite, J. H. Protein- and metal-dependent interactions of a prominent protein in mussel adhesive plaques. *J. Biol. Chem.* **2010**, *285* (33), 25850–25858.
- (14) Zhao, H.; Robertson, N. B.; Jewhurst, S. A.; Waite, J. H. Probing the adhesive footprints of *Mytilus californianus* byssus. *J. Biol. Chem.* **2006**, *281* (16), 11090–11096.
- (15) (a) Israelachvili, J.; Min, Y.; Akbulut, M.; Alig, A.; Carver, G.; Greene, W.; Kristiansen, K.; Meyer, E.; Pesika, N.; Rosenberg, K.; Zeng, H. Recent advances in the surface forces apparatus (SFA) technique. *Rep. Prog. Phys.* **2010**, *73* (3), -. (b) Lin, Q.; Gourdon, D.; Sun, C. J.; Holten-Andersen, N.; Anderson, T. H.; Waite, J. H.; Israelachvili, J. N. Adhesion mechanisms of the mussel foot proteins mfp-1 and mfp-3. *Proc. Natl. Acad. Sci. U.S.A.* **2007**, *104* (10), 3782–3786.
- (16) (a) Nakata, K.; Fujishima, A. TiO₂ photocatalysis: design and applications. *J. Photochem. Photobiol., C* **2012**, *13* (3), 169–189. (b) Jribi, R.; Barthel, E.; Bluhm, H.; Grunze, M.; Koelsch, P.; Verreault, D.; Sondergard, E. Ultraviolet irradiation suppresses adhesion on TiO₂. *J. Phys. Chem. C* **2009**, *113* (19), 8273–8277.
- (17) Lana-Villarreal, T.; Rodes, A.; Perez, J. M.; Gomez, R. A spectroscopic and electrochemical approach to the study of the interactions and photoinduced electron transfer between catechol and anatase nanoparticles in aqueous solution. *J. Am. Chem. Soc.* **2005**, *127* (36), 12601–12611.
- (18) Shoute, L. C. T.; Loppnow, G. R. Excited-state dynamics of alizarin-sensitized TiO₂ nanoparticles from resonance Raman spectroscopy. *J. Chem. Phys.* **2002**, *117* (2), 842–850.
- (19) (a) Frost, R. L.; Klopogge, J. T. Raman spectroscopy of the acetates of sodium, potassium and magnesium at liquid nitrogen temperature. *J. Mol. Struct.* **2000**, *526*, 131–141. (b) Liu, D.; Ullman, F. G.; Hardy, J. R. Raman-scattering and lattice-dynamic calculations of crystalline KNO₃. *Phys. Rev. B* **1992**, *45* (5), 2142–2147.
- (20) Wei, W.; Yu, J.; Broomell, C.; Israelachvili, J. N.; Waite, J. H. Hydrophobic enhancement of dopa-mediated adhesion in a mussel foot protein. *J. Am. Chem. Soc.* **2013**, *135* (1), 377–383.